Journal of Mechanical Design and Testing 5(1), (2023), 1-9
DOI: http://dx.doi.org/10.22146/jmdt.74006
e-ISSN: 2685-8029, ISSN: 2716-1293

Mechanical Properties and Corrosion Characteristics of Dissimilar Friction Stir Welded AA1000/AA6061-T6 Aluminum Alloys

C. Sokvisal and M.N. Ilman*

Departemen Teknik Mesin dan Industri, Fakultas Teknik, Universitas Gadjah Mada.
Jl. Grafika No. 2, Kompleks UGM, Yogyakarta 55281, Indonesia
e-mail: *ilman_noer@ugm.ac.id

Abstract

This paper is aimed to investigate microstructure, corrosion and mechanical properties of dissimilar metal weld joints between AA1000 and AA6061-T6 under different tool rotational speeds of 910, 1500, and 2280 rpm at a constant transverse speed of 30 mm/min. Several experimental works have been conducted including microstructure observation using optical microscopy and Scanning Electron Microscopy (SEM) equipped with Energy Dispersive X-ray Spectroscopy (EDS), Vickers microhardness measurements, tensile tests, and corrosion measurements using Potentiodynamic Polarization method. Results show that increasing tool rotational speed from 910 rpm to 1500 rpm increases the degree of homogeneity in nugget zone and improves strength of the weld joint but further increase in the tool rotational speed up to 2280 rpm degrades the mechanical properties due to coarsening of the microstructure. Furthermore, corrosion rate of the nugget zone (NZ) is in between the two base metals.

Keywords: Aluminum alloys, Friction Stir Welding, Dissimilar metals, Strengths, Corrosion.

Abstrak

Penelitian ini bertujuan untuk mempelajari perilaku struktur mikro, korosi dan sifat mekanis sambungan las tak sejenis antara aluminium padua AA1000 dan AA6061-T6 dengan variasi putaran tool 910, 1500 dan 2280 rpm pada kecepatan las 30 mm/menit. Beberapa pengujian yang dilakukan meliputi pengamatan struktur mikro menggunakan *Scanning Electron Microscopy* (SEM) yang dilengkapi dengan *Energy Dispersive X-ray Spectroscopy* (EDS), pengukuran kekerasan mikro Vickers, pengujian tarik dan pengujian korosi menggunakan metode *Potentiodynamic Polarization*. Hasil penelitian menunjukkan bahwa peningkatan kecepatan putaran tool dari 910 rpm ke 1500 rpm meningkatkan derajat homogenitas dan kekuatan sambungan las sedangkan peningkatan lanjut ke putaran 2280 rpm menurunkan sifat mekanis las karena pengasaran butir. Selanjutnya, hasil lainnya menunjukkan bahwa laju korosi las berada di antara kedua logam induk yang berbeda jenisnya.

Kata kunci : Aluminum paduan, *Friction Stir Welding*, Logam Tak Sejenis, Kekuatan Tarik, Korosi.

1. INTRODUCTION

Aluminum alloys have many desirable properties such as lightweight, high strength, good weldability and high corrosion resistance so that these alloys find many applications in indutries (T. A. Association, 1990; J. R. Davis, 2001). Due to their excellent properties as mentioned above, aluminum alloys either heat treatable and non-heat treatable are potentially recommended for engineering applications such as aluminum welded structures (H. Jamshidi Aval et al., 2012). However, some aluminum alloys such as 2xxx and 7xxx series can not be welded using conventional arc welding. The invention of friction stir welding (FSW) by The Welding Institute (TWI) in UK not only solves this problem but also enabling the dissimilar metals to be joined without cracking because this welding process is conducted in solid state condition below the melting point of both alloys to be joined (H. Mishra, R. and Sidhar, 2016). Friction stir welding (FSW) is welding technique in which the weld joint is produced by plunging a rotating tool into the butting edges of both metals followed by traveling of the tool along a weld line (W. M. Thomas et al., 1991). In this condition, heat is produced by frictional forces and the temperature is increased below the melting point.

In recent years, there have been many investigations aimed to study different parameters to improve the microstructure and mechanical properties of the friction stir dissimilar metal weld joints for aluminum alloys (W. B. Lee et al., 2003; P. Sadeesh et al., 2014). Rodriguez et al. (2015) have investigated microstructure and mechanical properties of dissimilar friction stir welding of AA6061 and AA7050 using butt joint with AA7050 was located at advancing side, whereas AA6061 located on the retreating side. In this study, the tool rotational speeds were varied of 270, 340, and 410 rpm at constant transverse speed of 114 mm/min by using a cylindrical threaded tool. The results revealed that FSW joints were marked by the presence of a band of mixed and unmixed materials based on different tool rotational speeds. In addition, the fracture of tensile test specimens was located at the nugget zone for low tool rotational speed and it was moved to the heat-affected zone (HAZ) for the higher speed due to the intermixing of materials. For another research, Zhang et al. (2019) also studied the microstructure and mechanical properties of similar and dissimilar AA7075 and AA2024 friction stir welding joint. This experiment was conducted with different tool rotational speed of 600, 950, 1300, and 1650 rpm and transverse speed of 100 mm/min. whereas the tool used had taper thread pin geometry. The results showed that the rotational speed had a significant influence on the mixing degree of dissimilar materials where the low tool rotational speed led to a limited material mixing. In contrast, high tool rotational speed produced union ring mixing pattern. It was found that the fracture location of all joints at different rotational speeds almost coincided with minimum hardness values of the corresponding joints.

Based on previous reports above, it can be seen that many research works related to the effect of tool rotational speeds of the welding process on microstructure and mechanical properties of dissimilar aluminum alloys have been conducted. However, there have been lack of data on friction stir dissimilar metal weld joints in particular AA1000 and AA6061-T6 aluminum alloys. Thus, this research is devoted to the investigation on microstructure and mechanical properties of friction stir dissimilar welded joints between AA1000 and AA6061-T6 aluminum alloys under different tool rotational speeds at constant transverse speed.

2. EXPERIMENTAL METHODS

2.1. Materials

The materials used in this investigation were AA1000 and AA6061-T6 plates with dimensions of 300 mm × 100 mm × 3 mm cut from the aluminum sheets. The chemical composition of AA1000 and AA6061-T6 aluminum alloys are shown in Table 1.

Table 1. Chemical Composition of AA1000 and AA6061-T6 (wt%)

Material	Mg	Si	Fe	Cu	Mn	Zn	Cr	Ti	Al
AA1000	0.081	0.122	0.256	0.179	0.024	0.024	0.003	0.020	Bal.
AA6061-T6	0.995	0.592	0.339	0.250	0.017	0.008	0.212	0.023	Bal.

2.2. Friction Stir Welding Process

Friction stir welding technique was selected for joining dissimilar AA1000 and AA6061-T6 wrought aluminum plates along 300 mm long with the welding direction was parallel to the rolling direction. In this experiment, AA1000 was located on the advancing side, whereas AA6061-T6 located on the retreating side as shown in Figure 1a. The welding was carried out using various tool rotational speeds of 910, 1500, 2280 rpm at constant transverse speed of 30 mm/s. During welding process, a cylindrical tool having a cylindrical pin was used and its geometry is shown in Figure 1b.

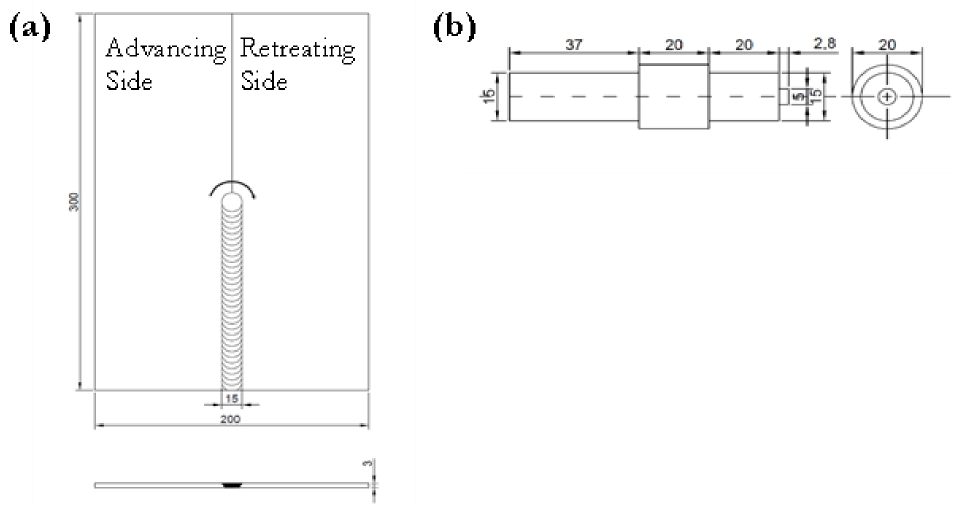

Figure 1. (a) Schematic of dissimilar FSW process, (b) Geometry of tool.

2.3. Metallurgical Examination

Macro- and microstructural examinations were carried out on the transverse section of the welds using optical microscopy. For the preparation, the weld samples for microstructure analysis were initially sectioned followed by grinding, polishing, and etching using Keller's reagent (2 ml HF + 3 ml HCl + 5 ml HNO_3 +190 ml H_2O). Apart from optical microscopy, other microstructural examinations using Scanning Electron Microscopy (SEM) and Energy Dispersive X-ray Spectroscopy (EDS) were also conducted with the samples were cut from the transverse section of the weld produced using the tool rotational speed 910 rpm. The size of the weld specimens for this metallographiy study was 5 mm × 3 mm × 5 mm.

2.4. Microhardness Measurements

The hardness measurements were conducted using Boehler Vickers microhardness testing on the cross section of the welded joints. The hardness measurement for each specimen was performed from the weld centerline toward HAZ and base metal using the load of 100 gf with dwell time of 10 s. The distance of indentation was set to 0.5 mm from point-to-point in the cross-section of center weld around 80 points.

2.5. Tensile Strength Measurements

The tensile tests were performed using a SHIMADZU servopulser testing machine. Samples were machined in the form of transverse weld specimens according to ASTM E8 with the dimensional geometry is shown in Figure 2. From this testing, yield strength and ultimate tensile strength were determined.

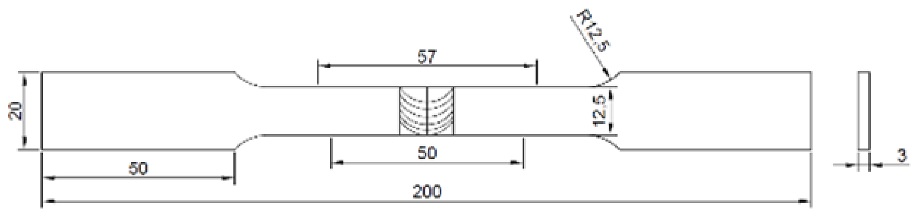

Figure 2. Tensile sample as following ASTM E8

2.6. Corrosion Rate Measurements

In this case, the corrosion rates was measured using potentiodynamic polarization method. For this investigation, samples were prepared in the form of circular-shaped specimens with diameter and thickness of 15 mm and 3 mm respectively. Each sample was taken from the different regions such as base metal of AA1000, base metal of AA6061-T6, and welded joint or nugget zone. Moreover, the samples were processed by grinding and polishing. Before testing, the electrolyte was prepared using distilled water of 965 ml and NaCl of 35 g to produce the 3.5% NaCl solution. The three-electrode cells used in this corrosion rate measurements was equipped with a cylindrical graphite rod used as the counter electrode and a saturated calomel reference electrode (SCE) whereas aluminum welded joints under study having exposed area of 0.5 cm² were positioned as a working electrode

3. RESULTS AND DISCUSSION

3.1. Microstructures

Microstructures of as received base materials, namely AA1000 and 6061-T6 aluminum alloys are shown in Figure 3. It can be seen that the microstructure of AA1000 in Figure 3a consists of elongated grains along the rolling direction with average grain size of 300 μm in length and 80 μm in width. Such a microstructure has been reported previously (, 2001). Based on the chemical compositions in Table 1, it is seen that AA1000 is pure aluminum alloy (non-heat treatable) which contains mostly aluminum element (Al) with its percentage is around 99.28%. Several elements with low percentages, typically below 0.72 wt. % are not considered as alloying elements. Figure 3b shows microstructure of AA6061-T6 marked by the presence of smaller grain size. In addition, the presence of fine precipitates are also observed in Figure 3b. According to the previous reports (P. Mukhopadhyay, 2012) these fine precipitates which are uniformly distributed in the microstructure of AA6061-T6 are composed of Mg and Si in the form of Mg_2Si. This is because AA6061-T6 is the heat treatable material in which its strength is produced due to T6 treatment which consists of solution heat-treated and artificial aged treatments.

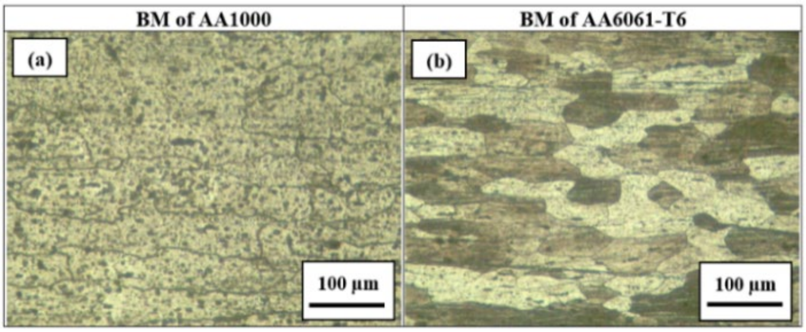

Figure 3. The base material of AA1000 and AA6061-T6

Figure 4 shows typical micro-structures of HAZ in AA1000 advancing side and AA6061-T6 retreating side with various tool rotational speeds 910, 1500, and 2280 rpm. The HAZ microstructures were slightly different to the base metals due to different processing. It is noticed that the HAZ microstructures for both sides show large equiaxed morphology as the tool rotational speed is increased due to temperature increase during the welding process (M. P. H. K. Pabandi and H. R. Jashnan, 2017).

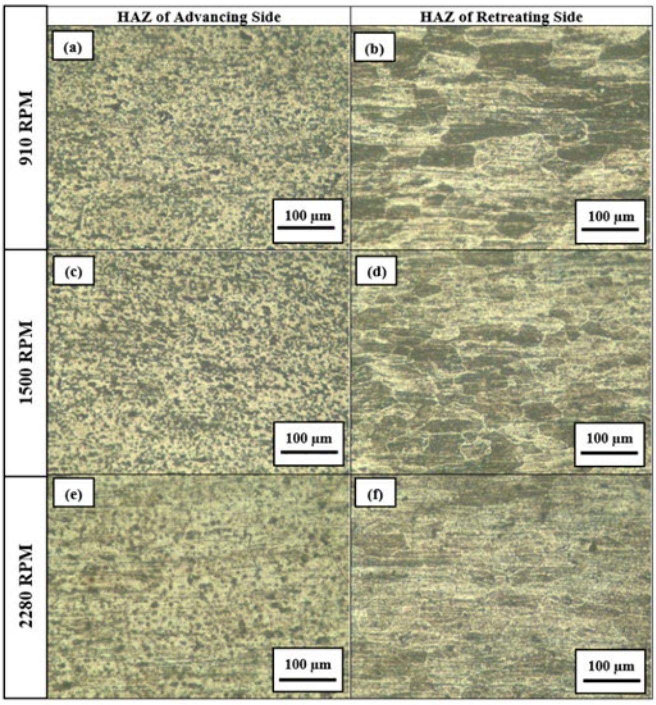

Figure 4. The HAZ of AA1000 and AA6061-T6

Figure 5 shows typical microstructures of different regions in friction stir welded joints, namely TMAZ/NZ of AA1000 side, NZ, and NZ/TMAZ side of AA6061-T6. These regions confirm the evidence of stirring process with different tool rotational speeds. Figure 6(a),(d),(g) indicate more clearly deformed and bent grains in TMAZ regions at the advancing side as a result of stirring process at high temperature leading to recrystallization (D. Devaiah et al., 2016). Subsequently, Figure 5(b),(e),(h) illustrate NZ regions often known as dynamically recrystallized zones (DRZ), which contain the equiaxed-fine-grains caused by creating the new structures from the stirring process. It is evident that increasing tool rotational speeds leads to coarser grains due to recrystallization and growth at high temperature (D. Devaiah et al., 2016). This is because high tool rotational speed increases frictional heat which in turn temperature in NZ. It is also seen that the increasing tool rotational speed tends to increase the degree of mixing between the two materials in the nugget regions due to higher material flow under higher tool rotational speeds. Thus, the degree of regions and uncompleted mixing are depended on the material flow resulted from high temperature and plastic deformations during the welding process (D. Devaiah et al., 2016). Figure 6(c), (f), and (i) also show the plastic deformation on the retreating side with different angle of grains at NZ-TMAZ boundary caused by various tool rotational speeds.

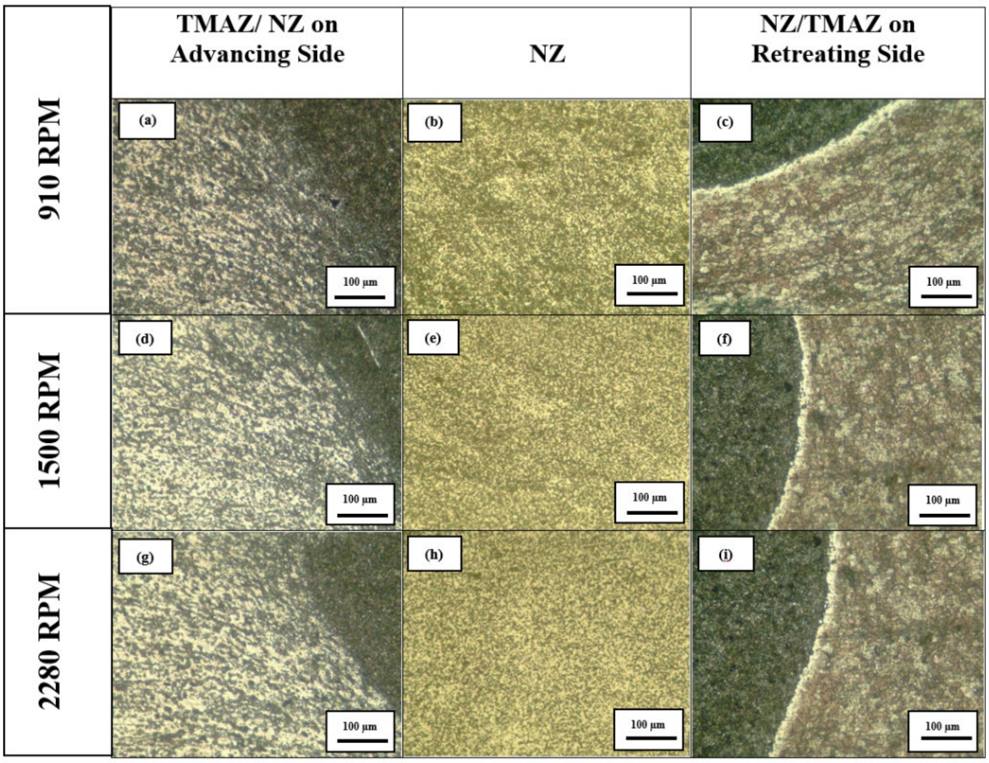

Figure 5. The welded zone of TMAZ/NZ, NZ, and NZ/TMAZ of AA1000 and AA6061-T6

To gain further information on the degree of mixing in NZ under various tool rotational speeds, macrostructure observations are also conducted and the results are shown in Figure 6. It can be seen that variations in NZ areas are resulted from different tool rotational speed of 910, 1500, and 2280 rpm. Etched macrographs also exposed the different material flow under various tool rotational speeds. From this examination, it is concluded that the nugget zone (NZ) for each weld has unsymmetrical inverted trapezoidal form which elongated at advancing side. The bright and dark regions in NZ are AA1000 and AA 6061-T6 respectively. This is because AA 1000 is more resistant to corrosion than AA1000 during etching (J. Yan, 2005). From Figure 6, it can be seen that under stirring action of tool, AA1000 material from advancing side penetrates toward the center of NZ and better mixing is observed as the tool rotational speed is increased (A. Rudolf, 2006).

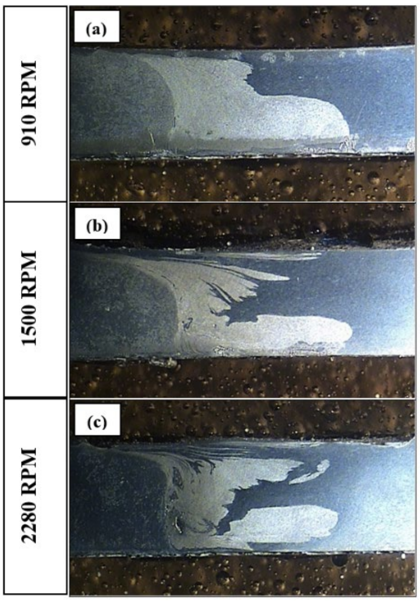

Figure 6. Macrostructure of various tool rotational speeds.

In order to examine distinct regions belong to AA1000 and AA6061-T6 aluminum alloys in NZ, SEM microanalysis equipped with EDS was conducted with the results are shown in Figure 7. In this study, the microstructural examination was focused on unseparated regions. Of note is that the locations in which the chemical compositions are identified using EDS are marked by a square. The magnified region marked by a square in Figure 7 are shown in Figure 8(a) with EDX-analysis for two different locations are given in Figure 8b,c,d. Referring to Table 2, it can be seen that EDX spectra named 001 and 002 taken from the bright region as seen in Figure 8a,b contain no Si suggesting that this region belongs to AA1000. In contrast, region marked 003 contains Si around 0.12% which is consistent with the composition of Al-Mg-Si alloy (AA6061-T6). Of note is that the percentage of C is higher, around 14.68% probably due contaminants during sample preparation whereas higher content of O is probably caused by oxidation. Therefore, these two elements are not considered to be alloying elements in aluminum alloys.

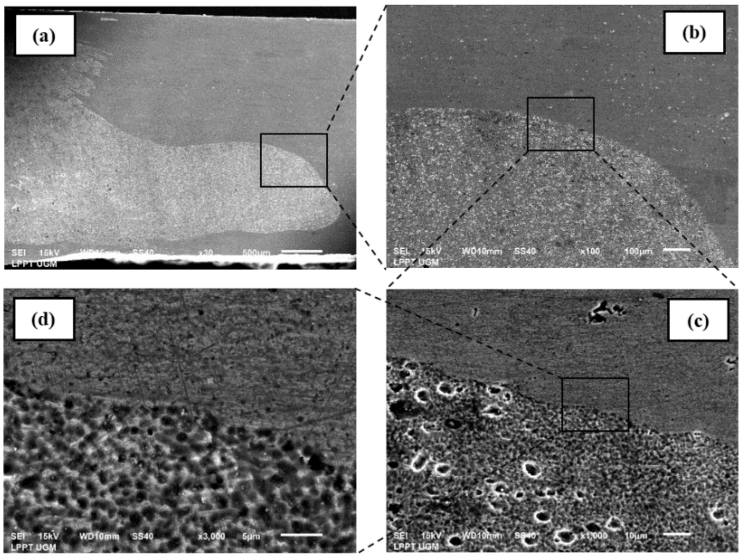

Figure 7. The configurations of SEM that located on the NZ of retreating side.

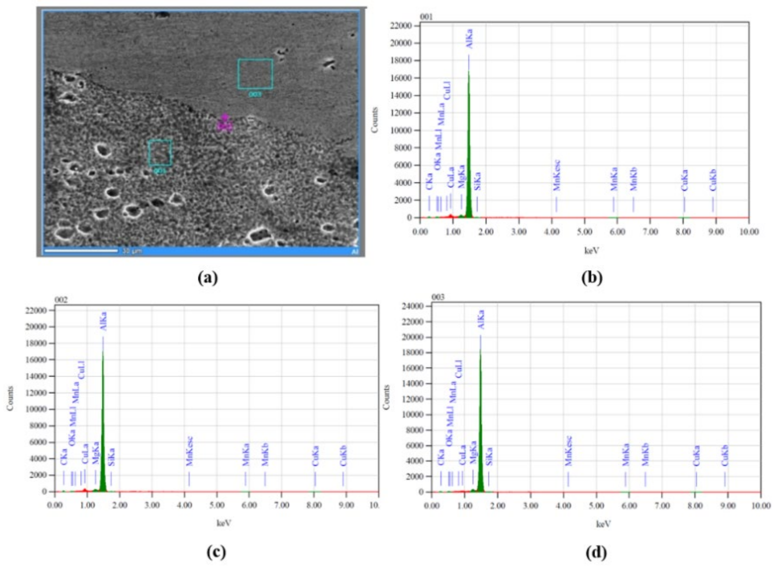

Figure 8. SEM image and EDS spectrums that showed the chemical compositions in different of three regions which located on the NZ of retreating side.

Table 2. EDS spectra values between NZ and TMAZ of AA6061-T6 aluminum alloy.

Element	Al	C	O	Mg	Si	Mn	Cu
Spectrum 001	80.28	14.68	1.72	0.82	-	0.51	1.98
Spectrum 002	79.35	16.29	1.22	0.50	-	0.55	2.09
Spectrum 003	85.53	11.52	1.33	0.73	0.12	0.04	0.74

3.2. Hardness Distributions

Figure 9 displays the hardness distribution profiles of various tool rotational speeds, namely 910, 1500, 2280 rpm. At low tool rotational speed, i.e. 910 rpm, the hardness peak value was observed in the NZ region adjacent to the AA1000 aluminum alloy retreating side wheras as the tool rotational speed is increased, the hardness peaks are moved towards the AA6061-T6 advancing side consistent with te previous work (M. M. Moradi et al., 2018). The plausible explanations are that the hardness peaks seen in Fig. 9 are associated with the occurrence of precipitation hardening due to AA6061-T6 metal in NZ. At a low tool rotational speed, i.e. 910 rpm, the frictional forces are not sufficient to transport AA6061-T6 from retreating side towards advancing side. In such a case as this, the hardness peak is found near AA6061-T6 retreating side. As the tool rotational speed is increased to 1500 rpm or higher (2280 rpm), much more AA6061-T6 are transported from retreating side to advancing side. As the results, the peaks of hardness move to the advancing side.

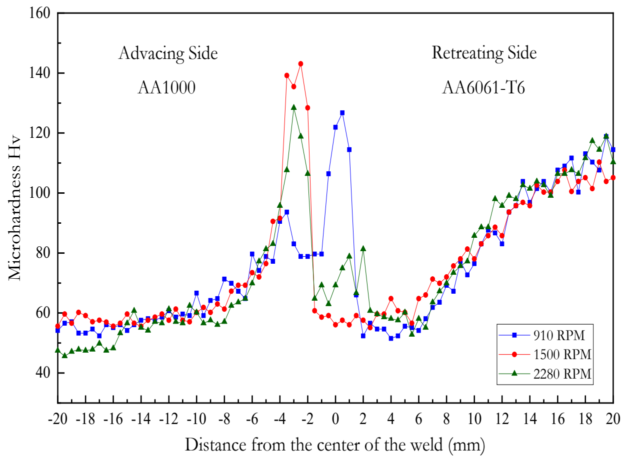

Figure 9. The hardness values of vaious tool rotaional speeds.

3.3. Tensile Strengths

Figure 10 presents to the tensile strength (TS), ultimate tensile strength (UTS) and elongation (E) of the various tool rotational speeds 910, 1500, 2280 rpm and constant transverse speed. Based on the results of the tensile testing, the tensile strength and ultimate tensile strength are slightly increase especially at 1500 rpm. The tensile strength and ultimate tensile strength of the weld at tool rotational speed 910 rpm is (UTS: 166.27 ± 3.43 MPa), (YS: 112.48 ± 5.16 MPa), (TE: 8.42 ± 0.52%) whereas 1500 rpm is (UTS: 169.29 ± 6.25 MPa), (YS: 116.77 ± 4.75 MPa), (E: 10. 91 ± 0.48%), and 2280 rpm is about (UTS: 168.07 ± 3.83 MPa), (YS: 113.05 ± 3.06 MPa), (E: 11.85 ± 0.24%). The strengths of the weld joints seem to be influenced by many factors such as grain size according to the Hall-Petch relationship which states that strength is inversely proportional to square root of grain size, the degree of mixing of two dissimilar metals in NZ and re-precipitation of AA6061-T6. In one hand, a low tool rotational such as 910 rpm produces finer grains in NZ which improves the strength but on the other hand, the mixing of two dissimilar metals is not completely achieved at the low rotational speed due to insufficient friction forces. In addition, at low tool rotational speed of 910 rpm, re-precipitation of AA6061-T6 metal in NZ which improves the strength may not occur and in contrast, at a high tool rotational speed of 2280 rpm, softening is expected to occur due to over ageing. It seems that precipitation hardening is likely to occur at a medium tool rotational speed of 1500 rpm. These results seem to suggest that the optimum tool rotational speed is achieved at 1500 rpm owing to the best combination of grain size, the degree of mixing and re-precipitation.

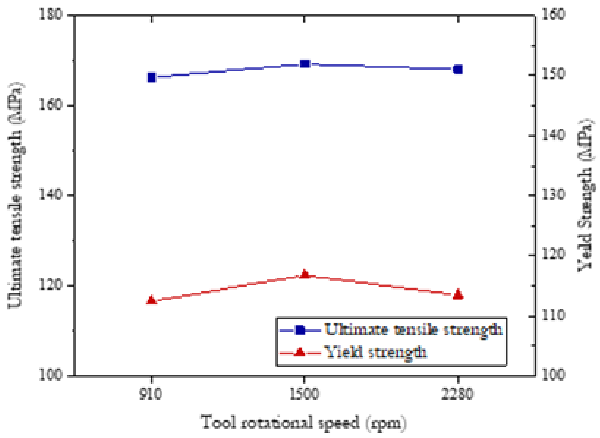

Figure 10. The tensile strength and yield strength with various tool rotational speeds.

3.4. Corrosion Rate Measurements

Figure 11 reveals the corrosion rate results obtained from the electrochemical test in the three regions such as base metal of AA1000, the base metal of AA6061-T6 and welded joint in NZ of both aluminum alloys.

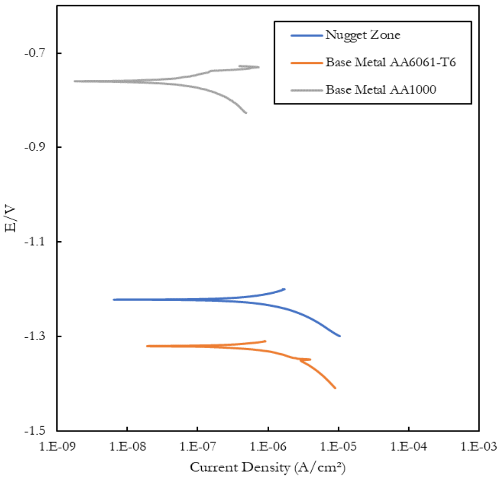

Figure 11. Potentiodynamic polarization curves of FSW dissimilar weld and two base metals.

The base metal of AA1000 has a very good resistance of corrosion if it compared with two other samples. This is because AA1000 is pure aluminum that consists of a higher percentage of Al (99.28%) and it has a capability of forming passive film. The corrosion rate in NZ falls within the two base metals as reported previously (A. Kumar et al., 2017; C. Shen et al. 2011).

4. CONCLUSION

In this investigation, we have experimentally investigated the effects of various tool rotational speeds of dissimilar friction welded joint between AA1000 and AA6061-T6 on macro and microstructures, microhardness, tensile strengths, and corrosion rates. The following conclusions can be drawn from the experimental results as below:

- The microstructures of friction stir weld joints in HAZ, TMAZ, and NZ are strongly influenced by tool rotational speeds. The increase in the tool rotational speed leads to an increase in the dynamic recrystallization of grain in the NZ. In addition, increasing tool rotational speed increase material flow which can cause complete mixing due to the high deformation by stirring of the tool. Results of macrostructure examinations confirm the formation of onion rings at higher tool rotational speed.
- The peaks of microhardness in the NZ are shifted from the region near retreating side (AA6061-T6) towards the regions close to advancing side (AA1000). These behaviors are related to the degree of mixing due to stirring action of pin.

- Increasing tool rotational speed achieve a maximum value at 1500 rpm whereas higher speed to loss of strength. Similar results are observed for yield strength. It seems that the strength of the weld joints under study are associated with the grain size according to Hall-Petch equation.

The best corrosion resistance is observed in AA1000 base metal marked by high potential and low corrosion density. In contrast, AA6061-T6 show the worst corrosion performance due to the presence of alloying elements such as Mg and Si. The corrosion rate of the dissimilar A1000/AA6061-T6 is between the two base metals.

5. ACKNOWLEDGEMENT

We acknowledge the financial support from the KNB Dikti scholarship program. Also thankful to UGM that have given the laboratory of all tests for completed successfully.

6. REFERENCES

A. Kumar, S. K. Sharma, K. Pal, and S. Mula, "Effect of Process Parameters on Microstructural Evolution , Mechanical Properties and Corrosion Behavior of Friction Stir Processed Al 7075 Alloy," J. Mater. Eng. Perform., vol. 26, no. 3, pp. 1122–1134, 2017.

A. Rudolf, Extrusion of semifinished products in aluminum alloys. 2006.

C. Shen, J. Zhang, and J. Ge, "Microstructures and electrochemical behaviors of the friction stir welding dissimilar weld," J. Environ. Sci., vol. 23, no. SUPPL., pp. S32–S35, 2011.

C. Zhang, G. Huang, Y. Cao, Y. Zhu, and Q. Liu, "On the microstructure and mechanical properties of similar and dissimilar AA7075 and AA2024 friction stir welding joints: Effect of rotational speed," J. Manuf. Process., vol. 37, no. December 2018, pp. 470–487, 2019.

D. Devaiah, D. K. Kishore, and D. P. Laxminarayana, "Effect of Material Location and Tool Rotational Speed on the Mechanical Properties of Dissimilar Friction Stir Welded Aluminum Alloys (5083-H321to 6061-T6)," Bonfring Int. J. Ind. Eng. Manag. Sci., vol. 6, no. 4, pp. 186–190, 2016.

H. Jamshidi Aval, S. Serajzadeh, N. A. Sakharova, A. H. Kokabi, and A. Loureiro, "A study on microstructures and residual stress distributions in dissimilar friction-stir welding of AA5086-AA6061," J. Mater. Sci., vol. 47, no. 14, pp. 5428–5437, 2012.

H. Mishra, R. and Sidhar, Friction Stir Welding of 2XXX Aluminum Alloys Including Al À Li Alloys Friction Stir Welding of 2XXX Aluminum Alloys Including Al À Li Alloys A Volume in the Friction Stir Welding and Processing Book Series. 2016.

J. R. Davis, "Aluminum and Aluminum Alloys," in Light Metals and Alloys, ASM International, 2001, pp. 351–416.

J. Yan, M. A. Sutton, and A. P. Reynolds, "Process-structure-property relationships for nugget and heat affected zone regions of AA2524-T351 friction stir welds," Sci. Technol. Weld. Join., vol. 10, no. 6, pp. 725–736, 2005.

M. M. Moradi, H. Jamshidi Aval, R. Jamaati, S. Amirkhanlou, and S. Ji, "Microstructure and texture evolution of friction stir welded dissimilar aluminum alloys: AA2024 and AA6061," J. Manuf. Process., vol. 32, pp. 1–10, 2018.

M. P. Hossein Karami Pabandi, Hamid Reza Jashnan, "Effect of precipitation hardening heat treatment on mechanical and microstructure features of dissimilar friction stir welded AA2024-T6 and AA6061-T6 alloys," 2017.

P. Mukhopadhyay, "Alloy Designation, Processing, and Use of AA6XXX Series Aluminium Alloys," ISRN Metall., vol. 2012, no. Table 1, pp. 1–15, 2012.

P. Sadeesh et al., "Studies on friction stir welding of aa 2024 and aa 6061 dissimilar metals," Procedia Eng., vol. 75, pp. 145–149, 2014.

R. I. Rodriguez, J. B. Jordon, P. G. Allison, T. Rushing, and L. Garcia, "Microstructure and mechanical properties of dissimilar friction stir welding of 6061-to-7050 aluminum alloys," Mater. Des., vol. 83, pp. 60–65, 2015.

T. A. Association, "Rolling Aluminum : From the Mine Through the Mill on the Sheet and Plate Division ' s Technology Committee," p. 135, 1990.

W. B. Lee, Y. M. Yeon, and S. B. Jung, "The mechanical properties related to the dominant microstructure in the weld zone of dissimilar formed Al alloy joints by friction stir welding," J. Mater. Sci., vol. 38, no. 20, pp. 4183–4191, 2003.

W. M. Thomas;, N. J. C., and Needham, "Friction Stir Butt Welding," 1991.